Int. J. Chem. Sci.: 6(3), 2008, 1385-1398

MATHEMATICAL MODELLING OF HYDROGEN PRODUCTION SYSTEM IN FUEL CELL TECHNOLOGY

M. N. MURAT[a] and S. M. SAPUAN[*]

[a]School of Chemical Engineering, University Science Malaysia, Transkrian,
Nibong Tebal, PENANG, MALAYSIA
Department of Mechanical and Manufacturing Engineering, Universiti Putra Malaysia 43400 UPM
Serdang, SELANGOR, MALAYSIA

ABSTRACT

A fuel cell unit requires fuel to generate electricity. Hydrogen is seemed to be the ideal candidate as fuel due to its potential as an 'energy carrier'. In this paper, a model for hydrogen production system was proposed based on the experiments conducted in a packed bed reactor. Liquid methylcyclohexane (MCH) was used as a hydrogen carrier as it is easier to store or transport. A one-dimensional pseudo homogeneous fixed bed reactor model with axial mixing effects was chosen as a suitable solution to model the hydrogen production system. In order to solve the resulting model equations, the Finite Difference (FD) scheme was used to transform the equations into a discrete model, which is defined on a uniform grid points. The discrete model was successfully solved using Newton's method by means of a developed computer programme based on Fortran programming language. With the optimised model parameters, the simulation results show a good agreement with the experimental data. Therefore, the model can be considered successfully verified and further simulations with different operating conditions can be performed to study the performance of the hydrogen production system.

Key words : Hydrogen fuel, Fuel carrier, Mathematical modelling, Finite difference

INTRODUCTION

A fuel cell is an energy conversion device capable of converting the chemical energy from gaseous fuel directly into electricity through electrochemical combination process of the fuel with an oxidant[1-3]. In principle, a fuel cell operates similar to a battery but it does not need to be recharged. As long as fuel and oxidant are continuously supplied, a fuel cell is able to generate continuous power supply.

Attempts to develop fuel cells as successful practical power sources have been

[*] Author for correspondence; sapuan@eng.upm.edu.my

made over many years. Initially, fuel cells were developed mainly for the space and defence applications[1]. After this, further research has been carried out and fuel cells have recently attracted new attention due to their potential for the use in stationary and distributed electric power stations as well as transportation applications[2].

The importance of hydrogen is very much linked to the development of fuel cells. Almost all potential fuel cells technology utilise hydrogen as fuel, either in its pure form or in other forms. Hydrogen has been regarded as potential source of energy, or some researchers would prefer to call it 'energy carrier' instead, because of the nature of hydrogen that needs to be generated rather than freely available. With the ever increase in energy demand, hydrogen might be the best choice to be utilised as an energy carrier in order to balance the dwindling source of fossil fuel.

Hydrogen is considered as potential candidate for energy carrier because of the following advantages[4, 5].

- Hydrogen is one of the most abundant elements in the universe.
- Hydrogen is a sustainable form of energy in that it can be produced from many primary sources such as fossil fuels, renewable energy and nuclear power.
- Hydrogen is ideal for use in fuel cells to generate electricity.
- In fuel cell operation, hydrogen reacts with oxygen to produce pure clean water and no other pollutants are formed.
- Hydrogen is colourless, odourless, tasteless and non-toxic.

Mathematical model

Hydrogen can be produced in a packed bed reactor by the dehydrogenation of methylcyclohexane (MCH) in the presence of a catalyst (Pt/Al_2O_3). This process is also known as the MTH cycle (MCH-Toluene-Hydrogen cycle).

$$\underset{\text{MCH}}{C_7H_{14}} \longrightarrow \underset{\text{Toluene}}{C_7H_8} + \underset{\text{Hydrogen}}{3\,H_2} \qquad \ldots(1)$$

The experimental equipment used for the hydrogen production reactor is schematically presented in Fig. 1. The reactor is positioned vertically with the feed introduced from the top and the product coming out from the bottom of the reactor. The

geometry of the reactor used is an annular type, with empty space along its centre. This empty space is utilised for measuring temperature using a moveable thermocouple.

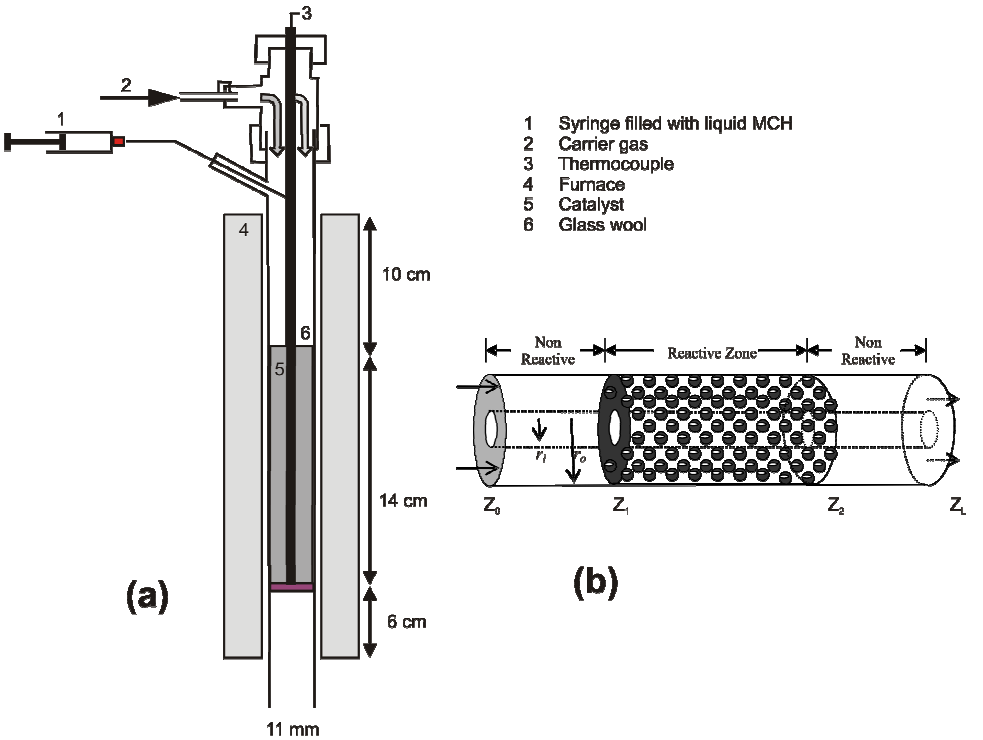

Fig. 1 : Schematic representation of hydrogen production reactor

Material balance equations -

Material balance equation used in the study is given in eq. (2).

$$\varepsilon \frac{\partial C}{\partial t} = \varepsilon D_{ea} \frac{\partial^2 C}{\partial z^2} - \varepsilon \frac{\partial (uC)}{\partial z} - \rho_b r \qquad \textbf{(reactive section)} \qquad \textbf{…}(2)$$

where :

ε = Catalyst void fraction

ρ_b = Catalyst bulk density (kg m^{-3})

C = Concentration of MCH (kg m^{-3})

D_{ea} = Effective (axial) diffusivity ($m^2\ s^{-1}$)

r = Rate of reaction (homogeneous model),

t = Time (s)

u = Velocity of fluid ($m\ s^{-1}$) and

z = Coordinate in axial direction (m).

The steady state material balance in the reactive section can be written as :

$$\varepsilon D_{ea}\frac{d^2C}{dz^2}-\varepsilon\frac{d(uC)}{dz}-\rho_b r=0 \qquad \ldots(3)$$

The steady state material balance in the non-reactive section :

$$D_f\frac{d^2C}{dz^2}-\frac{d(uC)}{dz}=0 \qquad \ldots(4)$$

where D_f = Fluid diffusivity ($m^2\ s^{-1}$)

Energy balance equations

The reactive section of energy balance equation is given in Eq. (5).

$$\bar{\rho}\bar{C}_p\frac{\partial T}{\partial t}=\lambda_{ea}\frac{\partial^2 T}{\partial z^2}-\rho_f C_{pf}\frac{\partial(uT)}{\partial z}+(-\Delta H)\rho_b r+\frac{2h_{wr}}{r_o}(T_o-T) \qquad \ldots(5)$$

where :

$\bar{\rho}$ = **A**verage density for both solid and fluid ($kg\ m^{-3}$),

λ_{ea} = Effective (axial) conductivity ($W\ m^{-1}\ K^{-1}$),

ρ_f = Density of fluid ($kg\ m^{-3}$),

ΔH = Heat of reaction ($J\ mol^{-1}$),

$\bar{C}_p$ = Average heat specific for both; solid and fluid ($J\ kg^{-1}\ K^{-1}$),

h_{wr} = Heat transfer coefficient along the wall (reactive) ($W\ m^{-2}\ K^{-1}$),

r_o = Outer radius (m),

T = Temperature (K) and

T_o = Temperature of the outer wall (K).

The steady state energy balance in the reactive section can be written as :

$$\lambda_{ea}\frac{d^2T}{dz^2}-\rho_f C_{pf}\frac{d(uT)}{dz}+(-\Delta H)\rho_b r + \frac{2h_{wr}}{r_o}(T_o-T)=0 \qquad \ldots(6)$$

The steady state energy balance in the non-reactive section :

$$\lambda_f\frac{d^2T}{dz^2}-\rho_f C_{pf}\frac{d(uT)}{dz} + \frac{2h_w}{r_o}(T_o-T)=0 \qquad \ldots(7)$$

where :

λ_f = Thermal conductivity of fluid (W m^{-1} K^{-1}),

C_{pf} = Specific heat of fluid (J kg^{-1} K^{-1}) and

h_w = Heat transfer coefficient along the wall (non reactive) (W m^{-2} K^{-1}).

Initial and boundary conditions

The model equations require initial and boundary conditions to be specified prior to obtaining the solution. The initial conditions are the condition of the system at initial time, i. e. at t = 0.The boundary conditions are the condition of the system at specific location of the boundary.

The initial conditions at time t = 0 are given in Eq. (8).

$$\begin{aligned} C\,(0, z) &= 0 \qquad (0 \le z \le L) \\ T\,(0, z) &= T_0 \qquad (0 \le z \le L) \\ U\,(0, z) &= 0 \qquad (0 \le z \le L) \end{aligned} \qquad \ldots(8)$$

The boundary conditions at the inlet (z = 0) are given in Eq. (9).

The fluid at the inlet of reactor is considered to have the same characteristic of the

feed :

$$C\ (t > 0,\ z = 0) = C_{in}$$
$$T\ (t > 0,\ z = 0) = T_{in}$$
$$U\ (t > 0,\ z = 0) = u_{in} \qquad \ldots(9)$$

The boundary conditions at the reactive interface ($z = z_1$) are discussed here. For a minimal thickness δ at the first boundary between non-reactive and reactive section (z_1), the flux entering the interface boundary is equal to the flux leaving the interface boundary. The flux consists of convective and conductive form of mass and heat transfer, respectively.

$$uC\big|_{z_1-\delta} - D_f \left.\frac{dC}{dz}\right|_{z_1-\delta} = uC\big|_{z_1+\delta} - D_{ea} \left.\frac{dC}{dz}\right|_{z_1+\delta} \qquad \ldots(10)$$

$$u\rho_f C_{pf} T_f\big|_{z_1-\delta} - \lambda_f \left.\frac{dT}{dz}\right|_{z_1-\delta} = u\rho_f C_{pf} T_f\big|_{z_1+\delta} - \lambda_{ea} \left.\frac{dT}{dz}\right|_{z_1+\delta} \qquad \ldots(11)$$

As $\delta \to 0$, the form of boundary conditions at the interface :

$$D_f \left.\frac{dC}{dz}\right|_{z_1-\delta} = D_{ea} \left.\frac{dC}{dz}\right|_{z_1+\delta} \qquad \ldots(12)$$

$$\lambda_f \left.\frac{dT}{dz}\right|_{z_1-\delta} = \lambda_{ea} \left.\frac{dT}{dz}\right|_{z_1+\delta} \qquad \ldots(13)$$

The boundary conditions above show that the changes occur at the interface boundary are due to the changes of the value of diffusivity coefficient and thermal conductivity as well as the changes in concentration and temperature gradients.

The boundary conditions at the exit ($z = z_2$) is given in Eq. (14).

$$\frac{dC}{dz} = \frac{dT}{dz} = 0 \qquad \ldots(14)$$

Kinetic model

There are a number of kinetic studies have been carried out for the dehydrogenation of methylcyclohexane in packed bed reactor[6-9]. However, the limited experimental data in the literature do not allow us to utilise the reported form of kinetic expression. Thus, we have to make simplification on the reported kinetic model in order to reduce the number of uncertainties in our model equation :

- Since the dehydrogenation reaction of MCH is very fast and highly endothermic[10], we assume that the reaction is irreversible.
- The reaction rate can be expressed in term of concentration, by introducing the ideal gas equation :

$$(P_i = \frac{n_i}{V} RT \, , \, C_i = \frac{n_i}{V})$$

- Reaction rate is evaluated at the catalyst surface conditions.
- Surface temperature of catalyst T_s is assumed constant at 643.15 K

Thus, relatively simple expressions can then be obtained :

$$r = k(RT_s)\ C\ s^{-1} \qquad \ldots(15)$$

$$k = A\exp\left(-\frac{E}{R}\frac{1}{T_s}\right)\exp\left(\frac{1}{650}\frac{E}{R}\right) \qquad \ldots(16)$$

where :

A = Pre-exponential factor,

E = Activation energy (J mol^{-1}),

n = Number of moles,

P = Pressure (Pa),

R = Universal gas constant (J mol^{-1} K^{-1}),

T_s = Surface temperature of solid catalyst (K) and

V = Volume (m^3).

Finite difference approximation

From the steady state mathematical model derivation, the resulting type of model equations is a second order differential algebraic equation. To solve these model equations, a Finite Difference (FD) approximation method is utilised. Fig. 2 shows a uniform grid representing one-dimensional geometry of hydrogen production reactor.

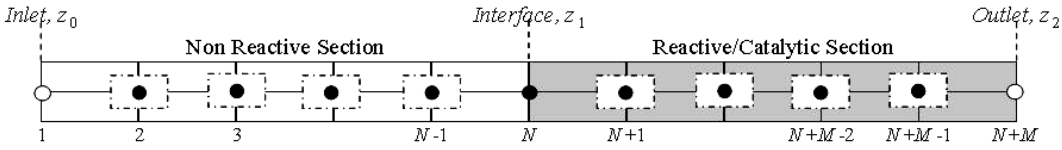

Fig. 2 : Uniform grid representation of hydrogen production reactor

For achieving higher accuracy while approximating, multiple points FD approximation is usually applied. The more points involved in approximating any variable at a certain point, the higher degree of accuracy will be obtained. The required weights in FD formulas can be obtained from the code provided by Fornberg[11-12]. These codes are very useful for evaluating the weights in FD formulas for different order of derivatives as well as order of accuracy.

First derivative approximation

At the point $i = 2$ and the point $i = N + 1$:

$$\left.\frac{dx}{dz}\right|_{x_i} \cong \frac{x_{i+1} - x_i}{\Delta z} \qquad \ldots(17)$$

where x representing each variable C, T or u.

At the point $i = 3$ and the point $i = N + 2$:

$$\left.\frac{dx}{dz}\right|_{x_i} \cong \frac{\frac{1}{6}x_{i-2} - x_{i-1} + \frac{1}{2}x_i + \frac{1}{3}x_{i+1}}{\Delta z} \qquad \ldots(18)$$

At points from $i = 4$ to $i = N - 1$ and points from $i = N + 3$ to $i = N + M–1$:

$$\left.\frac{dx}{dz}\right|_{x_i} \cong \frac{-\frac{1}{12}x_{i-3} + \frac{1}{2}x_{i-2} - \frac{3}{2}x_{i-1} + \frac{5}{6}x_i + \frac{1}{4}x_{i+1}}{\Delta z} \qquad \ldots(19)$$

At the point $i = N$:

$$\left.\frac{dx}{dz}\right|_{x_{N-\delta}} \cong \frac{-\frac{1}{3}x_{N-3} + \frac{3}{2}x_{N-2} - 3x_{N-1} + \frac{11}{6}x_N}{\Delta z_1} \qquad \ldots(20)$$

$$\left.\frac{dx}{dz}\right|_{x_{N+\delta}} \cong \frac{-\frac{22}{12}x_{N+3} + 3x_{N+2} - \frac{3}{2}x_{N+1} + \frac{1}{3}x_N}{\Delta z_2} \quad \ldots(21)$$

Here, totally *forward* FD approximation is used. This is because the model equation describing the non reactive section is changed at the point beyond $i = N$; thus, all previous points will not be valid for the new equation describing the reactive section. Therefore, the approximation has to be based on *forward* FD where all the points are in the reactive section.

Second derivative approximation

All the second derivatives are approximated by *centred* FD.

At the point $i = 2$ and $i = N + 1$:

$$\left.\frac{d^2x}{dz^2}\right|_{x_i} \cong \frac{x_{i-1} - 2x_{i+1} + x_{i+2}}{(\Delta z)^2} \quad \ldots(22)$$

At points from $i = 3$ to $i = N - 2$ and from $i = N + 2$ to $i = N + M–2$:

$$\left.\frac{d^2x}{dz^2}\right|_{x_i} \cong \frac{-\frac{1}{12}x_{i-2} + \frac{4}{3}x_{i-1} - \frac{5}{2}x_i + \frac{4}{3}x_{i+1} - \frac{1}{12}x_{i+2}}{(\Delta z)^2} \quad \ldots(23)$$

At the point $i = N - 1$ and $i = N + M–1$:

$$\left.\frac{d^2x}{dz^2}\right|_{x_i} \cong \frac{x_{i-1} - 2x_i + x_{i+1}}{(\Delta z)^2} \quad \ldots(24)$$

RESULTS AND DISCUSSION

As it can be seen from Fig. 3, the simulation results with the optimised parameter are generally in good agreement with the experimental results for hydrogen as carrier gas. The best fitting were obtained for 24.01 % organic load as shown in Fig. 3(d), whereby the simulation curve obtained touches most of the experimental points. The maximum temperature in the non-reactive section and the ‘cold spot’ temperature in the reactive section are well predicted.

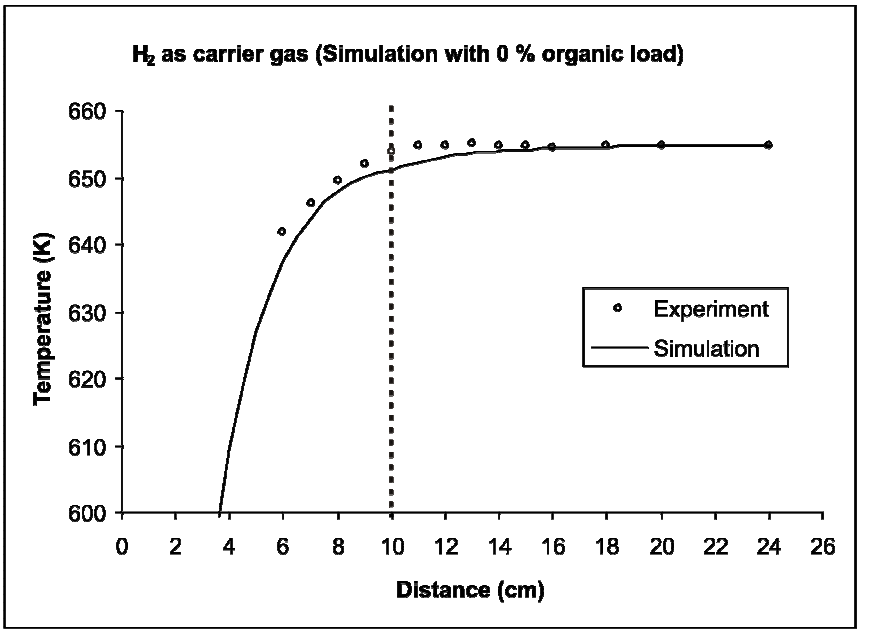
H2 as carrier gas (Simulation with 0 % organic load)
Temperature (K)
660
650
640
630
620
610
600
0 2 4 6 8 10 12 14 16 18 20 22 24 26
Distance (cm)
Experiment
Simulation

(a)

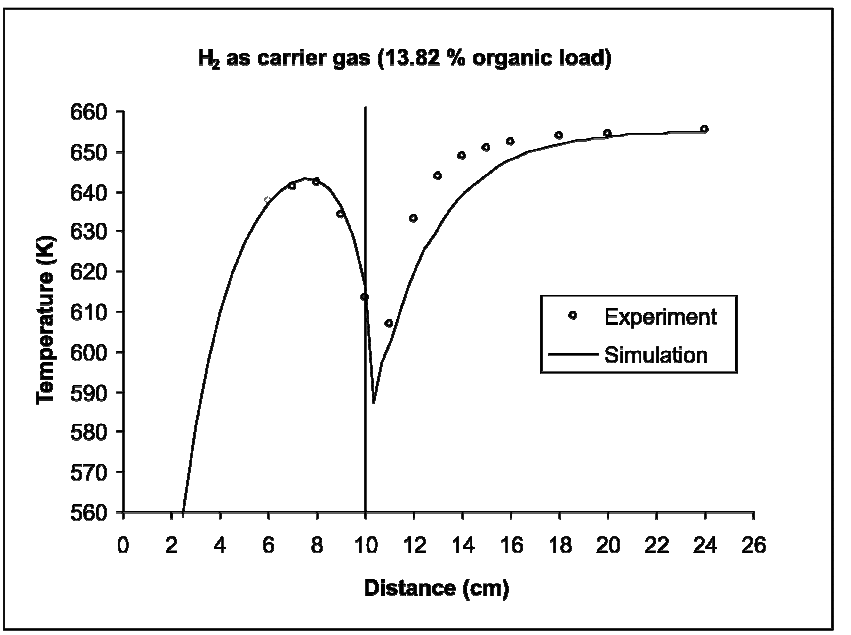
H2 as carrier gas (13.82 % organic load)
Temperature (K)
660
650
640
630
620
610
600
590
580
570
560
0 2 4 6 8 10 12 14 16 18 20 22 24 26
Distance (cm)
Experiment
Simulation

(b)

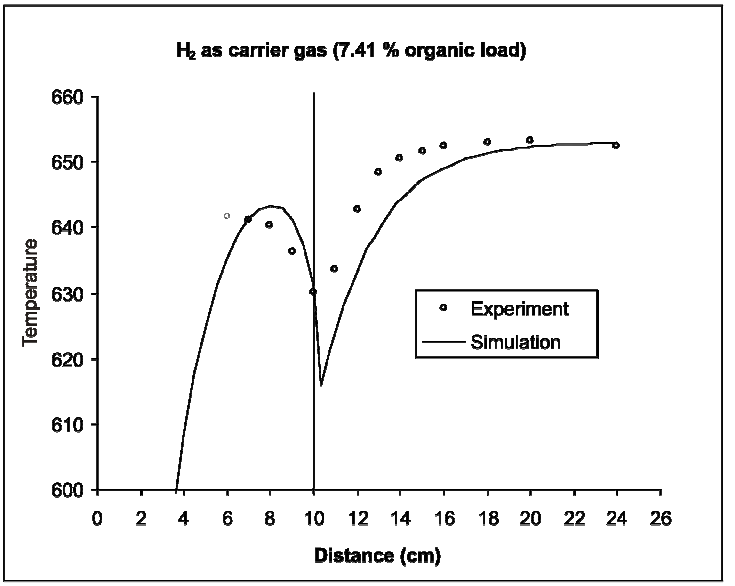

(c)

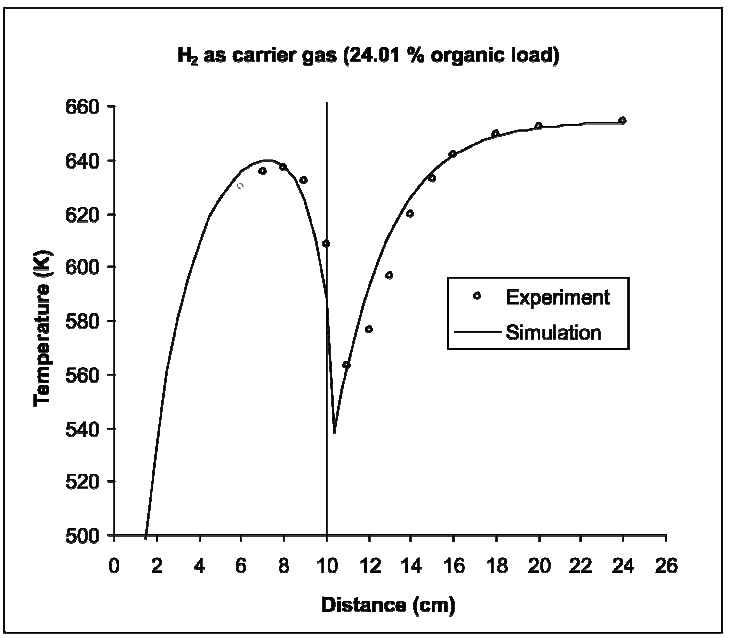

(d)

Fig. 3 : Comparison between simulation using optimised parameters and experimental results

Fig. 3(a) for no organic load also show good simulation results as compared to the experimental results. Most of the experimental data point located closely to the simulation curve.

Fig. 3(b) shows the results for organic load of 7.41 %. In this simulation, the results are not as good as expected. With low concentration of MCH (low percentage of organic load), the experimental observation shows more temperature fluctuation tends to occur, especially in the non-reactive section where no catalyst is present.

Fig. 3(c) shows simulation results with 13.82 % organic load. The results show a good agreement with the experimental results, especially in the non reactive section. However, the temperature profile in the reactive section shows slightly lowered value as compared to the experimental result. Both simulations with 7.41 % and 13.82 % organic load show similar results in the reactive section. The possible explanation for this could be due to heat transfer problems as a result of catalyst packing and the abrupt change in the organic concentration after reaction.

Looking at Fig. 3(c) and 3(d), there exist maximum curves where temperature start increasing to a maximum value and then gradually decrease as going near the reactive section. Both simulation and experimental results show this phenomenon. In Fig. 3(b) however, the experimental results do not clearly show as to how temperature start increasing from the entrance of the reactor, while the simulation results clearly do. Without more experimental data points available near the entrance of the reactor, it seems that the initial operating temperature was quite high.

In Fig. 3(b) and 3(c), the temperature profiles in the reactive section show slightly lowered value as compared to the experimental result. The possible explanation for this could be due to heat transfer problems as a result of catalyst packing and the abrupt change in the organic concentration after reaction. With higher organic load as shown in Fig. 3(d), the effect of reaction to reduce the organic concentration is less abrupt and thus, the simulation results are generally well agree with the experimental data.

Practically, the velocity of fluid is not constant throughout the reactor. Attempts to include a variable velocity have been made, but unfortunately, this has resulted in the serious numerical instability that it would not be possible to carry out further analysis such as parameter optimisation. According to Froment and Bischoff[13], accounting for the velocity profile explicitly complicates the computation in a serious way. Thus, a constant superficial velocity was used. The effective parameters (effective diffusivity and effective

conductivity), which implicitly account the effect of the velocity, were introduced into the model equations.

CONCLUSIONS

A one-dimensional pseudo homogeneous fixed bed reactor model accounting axial mixing effects was developed to simulate the experimental packed bed reactor for the production of hydrogen. The results from simulation of the proposed model indicate that a good description of the temperature profile was obtained. Thus, it can be concluded that one dimensional pseudo homogeneous model is sufficient to describe the performance of the hydrogen production system, with the reactor geometry as described by the experimental setup.

By applying finite difference (FD) scheme, the steady state continuous model consisting of second order differential algebraic equations (DAEs) were transformed into a discrete model defined on a uniform grid point. This discrete model consists of a set of non-linear equations was successfully and efficiently solved by Newton's method. In general, the hydrogen production system has been modelled successfully. The simulation results are in good agreement with the experimental results, showing the reliability of the proposed model equation especially when higher percentage of organic load is used. Thus, the validity of model equation has been successfully verified.

REFERENCES

1. S. P. S. Badwal and K. Foger, Solid Oxide Electrolyte Fuel Cell Review, Ceramics International, **22**, 257-265 (1996).
2. O. Yamamoto, Solid Oxide Fuel Cells, Fundamental Aspects and Prospects. Electrochimica Acta, **45**, 2423-2435 (2000).
3. P. Aguiar, C. S. Adjiman and N. P. Brandon, Anode-Supported Intermediate Temperature Direct Internal Reforming Solid Oxide Fuel Cell. I, Model-Based Steady-State Performance, J. Power Sources, **138**, 120-136 (2004).
4. D. A. J. Rand and R. M. Dell, the Hydrogen Economy, A Threat or an Opportunity for Lead–Acid Batteries, J. Power Sources, in Press, (2005)
5. B. Johnston and M. C. Mayo and A. Khare, Hydrogen, the Energy Source for the 21st Century, Technovation, **25**, 569-585 (2005).
6. T. Schildhauer, E. Newson and St. Müller, the Equilibrium Constant for the Methylcyclohexane – Toluene System, J. Catal., **198**, 355-358 (2001).

7. G. Maria, A. Marin, C. Wyss, S. Muller and E. Newson, Modelling and Scaleup of the Kinetics With Deactivation of Methylcyclohexane Dehydrogenation for Hydrogen Energy Storage, Chem. Eng. Sci., **51**, 2891-2896 (1996).

8. M. El-Sawi, F. A. Infortuna, P. G. L. Parmaliana, F. Frusteri and N. Giordano, Parameter Estimation in the Kinetic Model of Methylcyclohexane Dehydrogenation on A Pt-Al_2o_3 Catalyst By Sequential Experiment Design, The Chem. Eng. J., **42**, 137-144 (1989).

9. P. A. Van Trimpont, G. B. Marin and and G. F. Froment, Kinetics of Methylcyclohexane Dehydrogenation on Sulfided Commercial Platinum/Alumina and Platinum-Rhenium/Alumina Catalysts, Ind. and Eng. Chem. Fund., **25**, 544-553 (1986).

10. S. Tschudin, T. Shido, R. Prins and A. Wokaun, Characterisation of Catalysts Used in Wall Reactors for the Catalytic Dehydrogenation of Methylcyclohexane, J. Catal., **181**, 113-123 (1999).

11. B. Fornberg, Generation of Finite Difference Formulas on Arbitrarily Spaced Grids. Mathematics of Computation, **51**, 699-706 (1988).

12. B. Fornberg, Calculation of Weights in Finite Difference Formulas, Siam Review, **40**, 685-691 (1998).

13. G. F. Froment and K. B. Bischoff, Chemical Reactor Analysis and Design. 2nd Ed., Wiley, Chichester (1990)

Accepted : 31.05.2008